Fault-Tolerance of Five-Phase Induction Machines with Mixed stator winding Layouts: Torque Ripple Analysis

M. Muteba, *Member, IEEE*, D. V. Nicolae, Member, *IEEE*

***Abstract* - The mixed winding layouts proposed in this paper are obtained by combining double and triple layer (DTL) windings in stator slots. Previous work has touched upon on the ability of three-and five-phase induction machines (IMs) with mixed winding layouts to produce torque with less ripple contents. However, their advantage when operating under open-circuited faults is yet to be comprehensively reported. This paper presents the fault-tolerant ability of Five-phase Induction Machines (FPIMs) with mixed winding layouts to produce torque with less ripple contents. The windings are designed as 2-pole and chorded with one slot, thereafter referred to as "DTL-14/15" and when chorded with two slots, thereafter referred to as "DTL-13/15. The magnetic conditions in the FPIMs are analyzed using Finite Element Method (FEM). The results evidenced that the FPIMs with the proposed DTL-14/15 and DTL-13/15 chorded coils reduced the torque ripple by a margin of about 60 % while operating with open-circuited faults respect to FPIMs with conventional double layer (DL) winding of the same coil span and operating under the same conditions. The results also prove that there is a great correlation between FEM (simulation) and experimental results.**

***Keywords*— Induction machines, Fault-Tolerance, Five-phase, Mixt-winding arrangement, Torque ripple.**

I. Introduction

THE search for more cost effective and fault tolerant layouts drives design of electrical machines up to its limits. Moreover, the requirements of many applications both in industry and in the field of renewable energy conversion are though that traditional layouts are abandoned in favour of new topologies or new light in shed over older one [2]. For three-phase induction motors to continue operating under loss of one phase, a divided dc bus and neutral connection are required [7]. In other words, a zero sequence component is necessary to provide an undisturbed rotating magneto-motive force (MMF) after a phase is lost.

Due to their additional degrees of freedom, multi-phase (more than three) motors are potentially more fault tolerant than their three-phase counterparts [3], [4], [5]. The design aspects of the proposed mixed winding configurations have been reported in [1]. In this paper, a 2-kW, 4.5-A, 170-V/phase, 50-Hz, 2-pole, 5-phase IM with 30 stator slots and 33 rotor bars is used for simulation and experimental tests. Fig.1 (a) and Fig. 1 (b) depict the phase winding distribution in conventional DL-13/15 and mixed winding DTL-13/15 layouts, respectively.

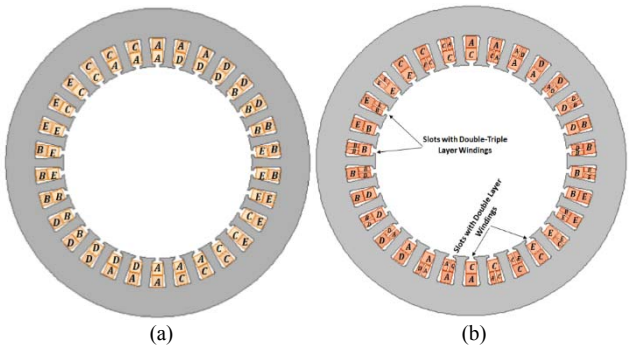

Fig.1. Five-phase winding distribution (a) Conventional DL-13/15, (b) Mixed Winding DTL-13/15

Each slot in the mixed winding layout "DTL-13/15" shown in Fig.1 (b) has conductors belonging to two different phases and each phase has four full coils and four half coils, all distributed in twelve slots under two poles. The current in these phases are out of phase with each other by either $4\pi/5$ or $6\pi/5$ electrical radian [1]. Elsewhere in the conventional DL-13/15 winding in Fig. 1 (a), each of ten slots have full coils belonging to the same phase and each of the other twenty slots accommodate coils that belong to two different phases. Therefore the net currents and leakage flux are less than for slots with current belonging to the same phase [1]. Again in a mixed winding DTL-14/15, only one slot per pole and per phase has current belonging to the same phase and three slots have current of two different phases which are out of phase. The phase band in the mixed winding layouts consists of four slots not three like in the conventional double layer winding, thus the phase-belt spread is $4\pi/15$ electrical radian in proposed mixed winding layouts and $\pi/5$ in the conventional double layer windings [1].

II. Fault-Tolerance of Five-Phase Windings

In this section the fault-tolerant scheme of the five-phase windings is explained. If one of the five phases is open circuited, the combination of phase current required to generate an undisturbed forward rotating MMF is no longer

M. Muteba is with the University of Johannesburg, Faculty of Engineering and Built Environment, Department of Electrical and Electronic Engineering Technology, PO Box 17001, Doornfontein, 2028, Johannesburg, South Africa. (e-mail: mmuteba@uj.ac.za).
D. V. Nicolae is with the University of Johannesburg, Faculty of Engineering and Built Environment, Department of Electrical and Electronic Engineering Technology, PO Box 17001, Doornfontein, 2028, Johannesburg, South Africa. (e-mail: danaurel@yebo.co.za).

978-1-4799-7940-0/15/$31.00 ©2015 IEEE

unique [8]. The most important consideration then is to establish an optimum set of currents which would produce the same value of MMF as under the healthy conditions.

Therefore, with proper current control, an undisturbed forward rotating MMF can be maintained, which can be used to control the electromagnetic torque [6]. The total stator MMF, F, of a five-phase machine can be formulated as in equation (1).

$$\vec{F} = NI_A + aNI_B + a^2 NI_C + a^3 NI_D + a^4 NI_E \quad (1)$$

Where, $a = 1\angle 72^o$, N is the number of turns per phase, I_A, I_B, I_C, I_D and I_E are the r.m.s stator currents of phase A, B, C, D and E, respectively. Under normal condition the MMF is written as in equation (2).

$$\vec{F} = \frac{5}{2} NI\ e^{j\theta} \quad (2)$$

Where, $\theta = \omega t + \varphi$ and φ is the phase shift.
When phase "A" is open-circuited, the real and imaginary parts of equation (2) are as in equations (3) [16].

$$\frac{5}{2} NI \sin\theta = N(I_B + I_E)\sin 72^o - N(I_C + I_D)\sin 36^o \quad (3)$$

To maintain the same value of F, the following should be fulfilled [16]; $I_B = -I_D$ and $I_C = -I_D$

III. Five-Phase IM Prototypes

A. Experimental Set up

A stator of a conventional three-phase squirrel cage induction machine was used to fit a two-pole five-phase distributed winding occupying 30 slots. The machines were fed from a five-phase synchronous generator. A M420 rotary type torque transducer with range from 0-50 Nm and 100 resolutions per second was used to measure the speed and torque strain in the rotary shaft. The Heenan air-cooled Eddy current break type with a stationary field with no slip rings or rotating transformers was used to load the different prototype machines.

B. FPIM Ratings, Dimensions and Parameters

To determine the magnetizing reactance "X_m" the machines were fed at rated frequency and rated voltage with Eddy current brake removed from the shaft. The machines rotate at speed closer to 3000 rpm which is the synchronous speed. The induced rotor current will be small as the speed of slip is very small. With approximate very small induced current, the stator current is very small. The rotor resistance "R_r", the stator and rotor leakage reactances "X_s and X_r" are determined using the locked rotor test, while the stator resistance "R_s" is determined using the conventional dc test. Table I gives the parameters of different prototype machines, while the detailed ratings and dimensions are given in Table II.

TABLE I
PROTOTYPE MACHINE PARAMETERS

Description	R_s	R_r	R_e	X_s	X_r	X_m
	All values are in Ohm					
DL-13/15	9.40	8.63	1403	7.96	7.96	130.19
DL-14/15	10.20	9.42	1130	8.25	8.25	151.08
DTL-13/15	9.05	8.23	1180	7.96	7.96	132.23
DTL-14/15	10.10	9.65	1215	7.66	7.66	159.48

TABLE II
PROTOTYPE MACHINE RATINGS AND DIMENSIONS

Description	Values
Rated phase voltage (V)	170
Rated line current (A)	4.5
Rated output power (kW)	2
Rated speed (rpm)	2800
Rated frequency (Hz)	50
No. of poles	2
No. of stator slots	30
No. of rotor bars	33
No. of turns per phase	198
Stator outer diameter (mm)	139.5
Stator internal diameter (mm)	93
Air-gap length (mm)	0.5
Stack length (mm)	120

IV. Finite Element Method

In this paper the finite element models are analyzed in nonlinear magneto-static problem based on the well-known Poisson's equation for vector magnetic potential well discussed in [9], [10], [11].
Electromagnetic torque has been computed from Maxwell's stress tensor. This method requires only the local flux density distribution along a specific line or contour and then the torque can be calculated by means of equation (4) [12].

$$T_e = r\left(\sum \frac{1}{\mu_o} B_n B_t\, d\right) l \quad (4)$$

Where B_n and B_t, are the normal and tangential components of the magnetic flux density, d is the length of the path between two consecutive nodes, r is the radius of the circular path taken and l is the axial length of the magnetic sheet core.
Based on the dimensions given in Table II, The Finite element models in Fig.2 and Fig.3 were built and simulated using the professional Quick Field software from Tera Analysis.

The flux density is assumed to lie in the plane of the model (x, y). The space current is described by the total number of ampere turns associated with the block density. Dirichlet boundary conditions with zero vector potential are set to the outer stator and inner rotor shaft of the machine models. By doing so, the solution is confined inside the machine frame
[13]. A two dimensional Cartesian-coordinate area are modelled with "r" number of nodes of mesh. Fig. 2 and Fig.3 depict how the flux density is distributed when the machines operate under healthy or open-circuited faulty conditions.

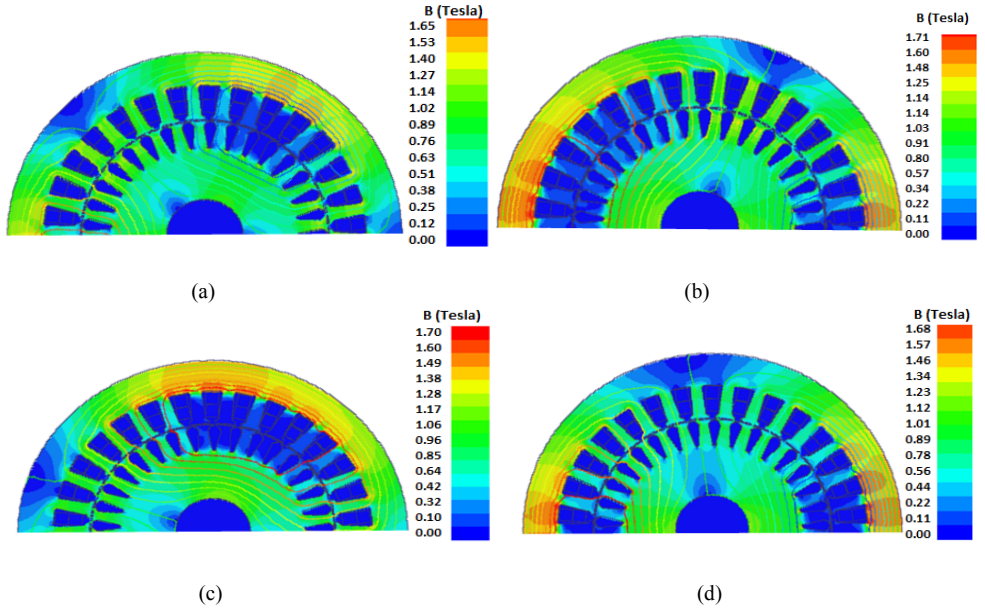

Fig.2. Finite-Element model results of flux density distribution for the five-phase machine with conventional DL-13/15 winding layout. (a) Healthy case. (b) Loss of phase A. (c) Loss of two adjacent phases and (d) Loss of two non-adjacent phases.

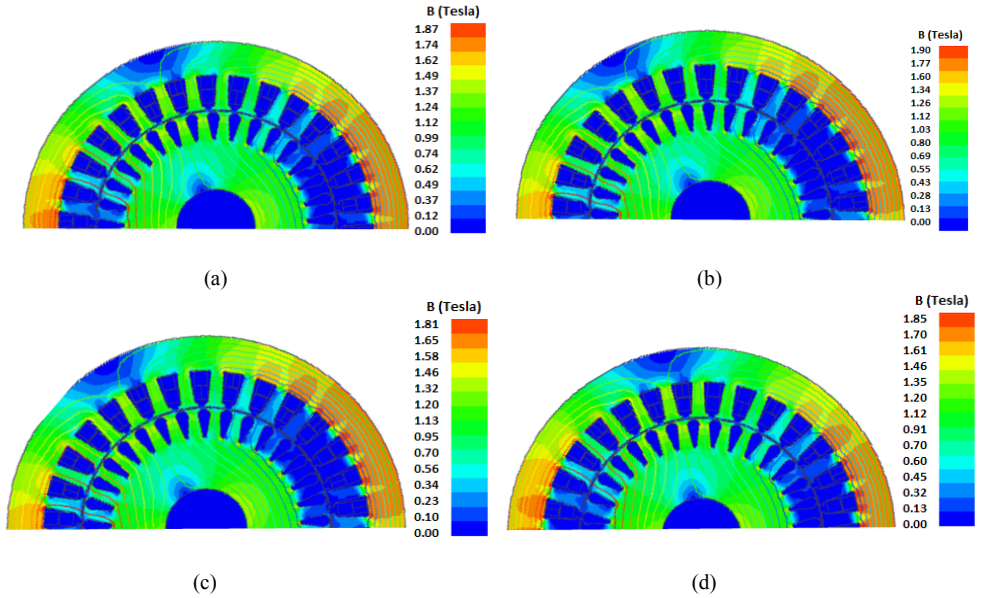

Fig.3. Finite-Element model results of flux density distribution for the five-phase machine with proposed DTL-13/15 winding layouts. (a) Healthy case. (b) Loss of phase A. (c) Loss of two adjacent phases and (d) Loss of two non-adjacent phases

V. Analysis of Results

A. Results for measured steady-state shaft torque

In Five-Phase Induction Machines, the primary sequence, mainly produces 1st, 9th, 11th, 19th, 21st, 29th, 31st, etc., space harmonics, while the secondary sequence, mainly produces the 3rd, 7th, 13th, 17th, 23th, 27^{th}, etc., space harmonics [1], [2], [14] . The first undesirable harmonics are the 9th and the 11th. The 11th harmonics was reduced because the prototype machine has 33 rotor bars, which is a multiple of 11. The bars are skewed by one slot pitch to cancel the effect of the 13th harmonics. The 19th and 21st will have a negligible effects on the machine. The 29th and 31st are slots harmonics and will contribute to high torque ripple.

Under full-load condition the five-phase IMs under analysis draw steady-state stator currents of 4.50 A. The torque is recorded in one second. The experimental torque profiles measured in time domain of FPIMs with conventional and proposed mixed winding layouts operating under healthy conditions are shown in Fig. 4 (a), (b), (c) and (d).

Under healthy operation the experimental torque profiles show constant oscillations of about f_T = 25 Hz for all machines. With loss of phase "A" the FPIM operates as an unbalanced four-phase induction machine, where two adjacent phases are out of phase by 144^o and the remaining phases are shifted from one another by 72^o electrical. The experimental torque profiles under loss of phase "A" are shown in Fig. 5 (a), (b), (c) and (d).

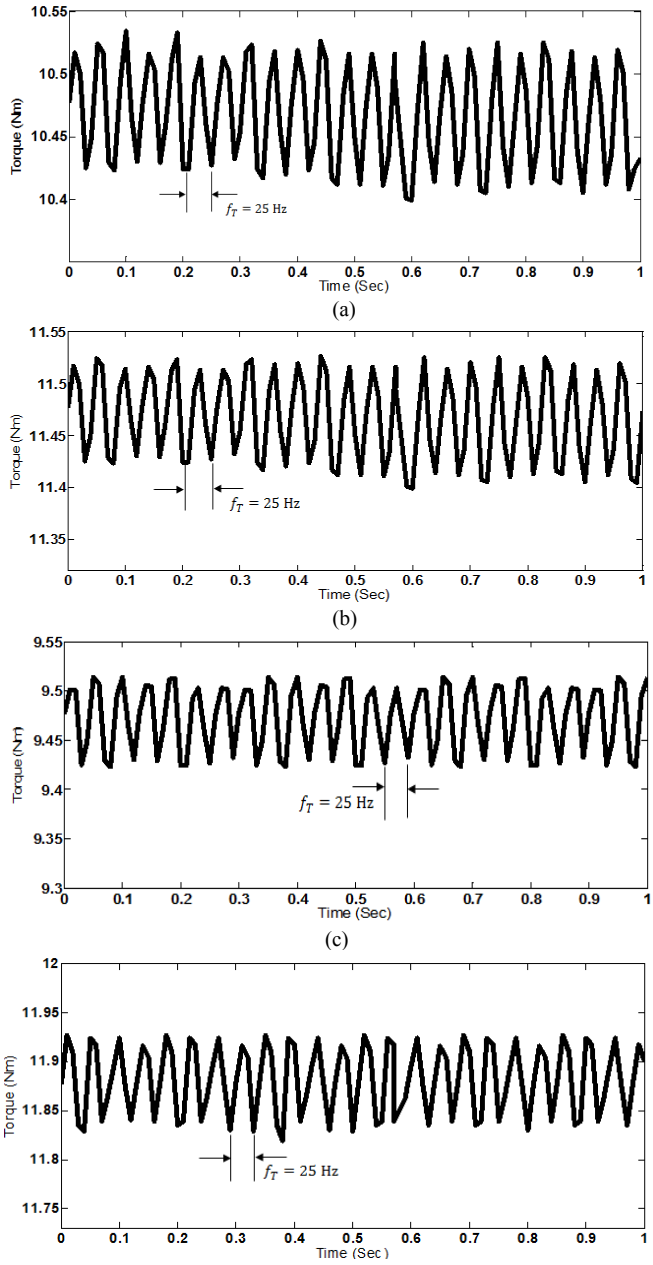

Fig.4. Experimental torque profile under healthy conditions, (a) DL-14/15, (b) DTL-14/15, (c) DL-13/15, (d) DTL-13/15

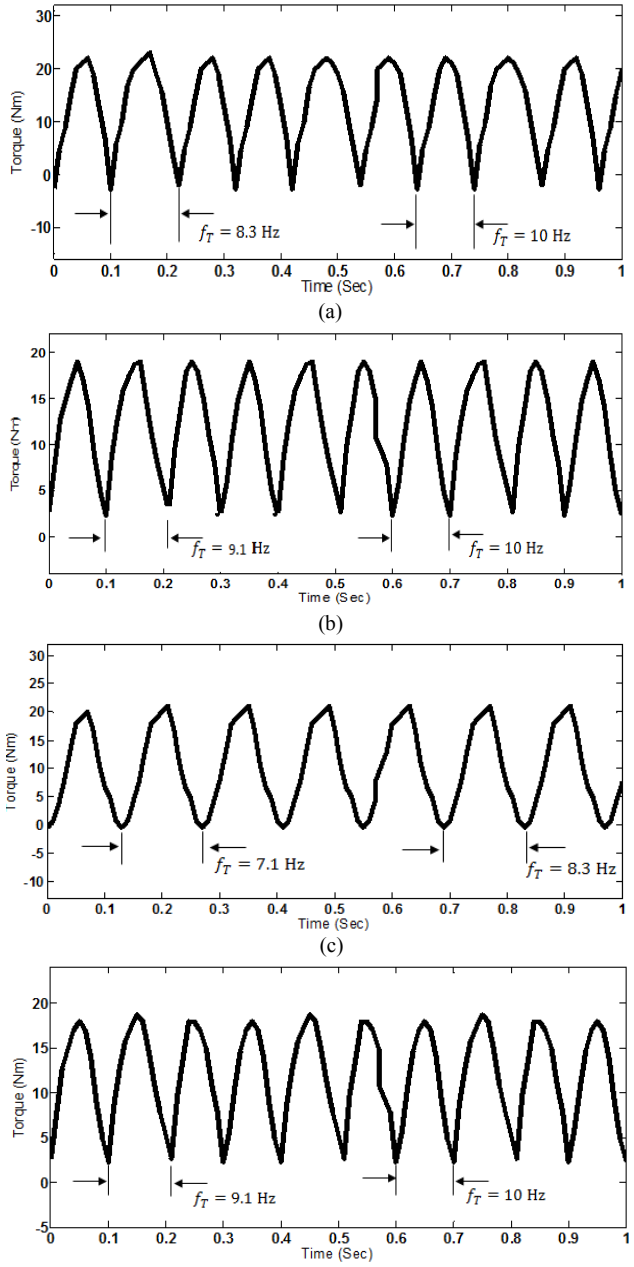

Fig.5. Experimental torque profile with loss of phase "A", (a) DL-14/15, (b) DTL-14/15, (c) DL-13/15, (d) DTL-13/15

With loss of "A" the oscillations are 8.3 Hz and 10 Hz for the conventional DL-14/15, and elsewhere the oscillations are 7.1 Hz and 8.3 Hz for the conventional DL-13/15. The corresponding oscillations for the proposed DTL-14/15 and DTL-13/15 are 9.1 Hz and 10 Hz in both machines.

The experimental torque profiles measured in time domain of FPIMs with conventional and proposed mixed winding layouts operating with loss of two adjacent phases separated by 72^o electrical are shown in Fig. 6 (a), (b), (c) and (d). Under this operation the FPIMs operate as unbalanced three-phase induction motors, where two adjacent phases are shifted by 216^o electrical and the remaining other adjacent phases are shifted from one another by 72^o electrical.

.

However, when a five-phase IM loses two non-adjacent phases separated by 144^o electrical, the machine operates as an unbalanced three-phase IM with two adjacent phases out of phase by 72^o electrical and other adjacent phases are out of phase by 144^o Electrical. Fig. 7 (a), (b), (c) and (d) show the experimental torque profiles measured in time domain of FPIMs with conventional and proposed mixed winding layouts operating with loss of two non-adjacent phases separated by 144^o electrical. With loss of two adjacent phases the experimental torque profiles show an oscillation 10 Hz for the conventional DL-14/15, and elsewhere for the conventional DL-13/15 the oscillations of about 11.1 Hz and 12.5 Hz were recorded.

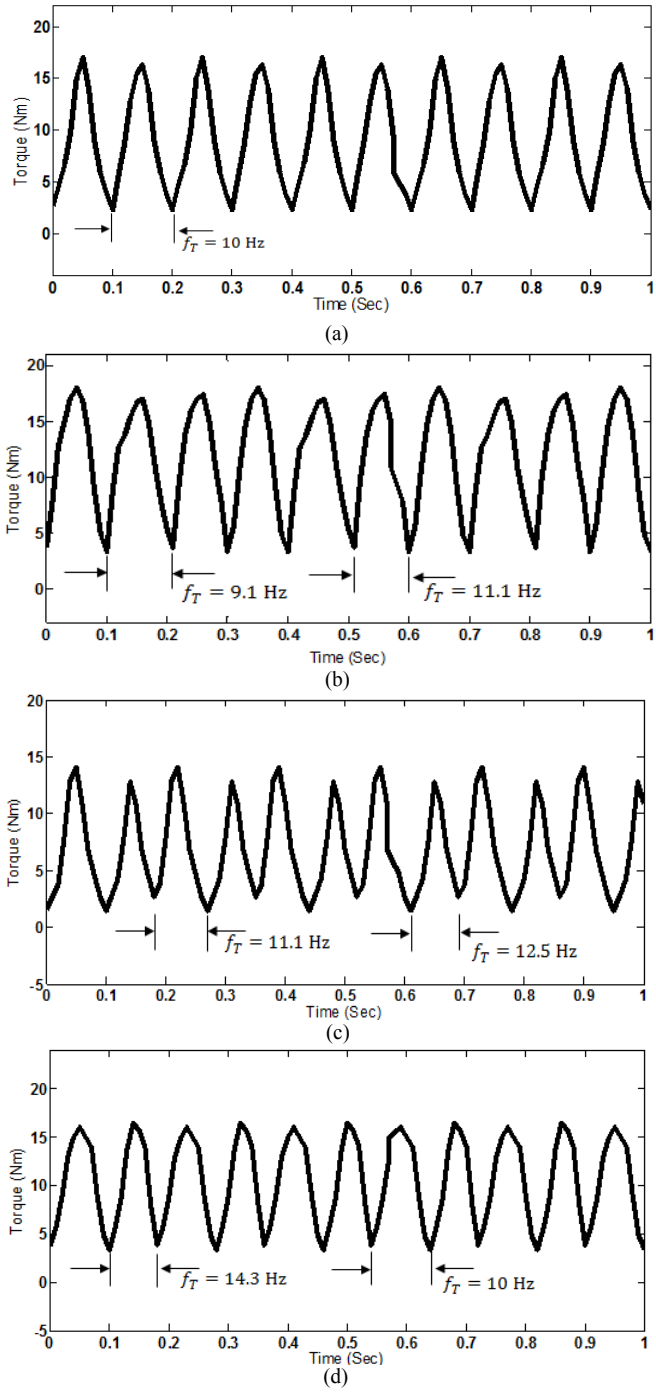

Fig.6. Experimental torque profile at full-load with loss of two adjacent phases, (a) DL-14/15, (b) DTL-14/15, (c) DL-13/15, (d) DTL-13/15

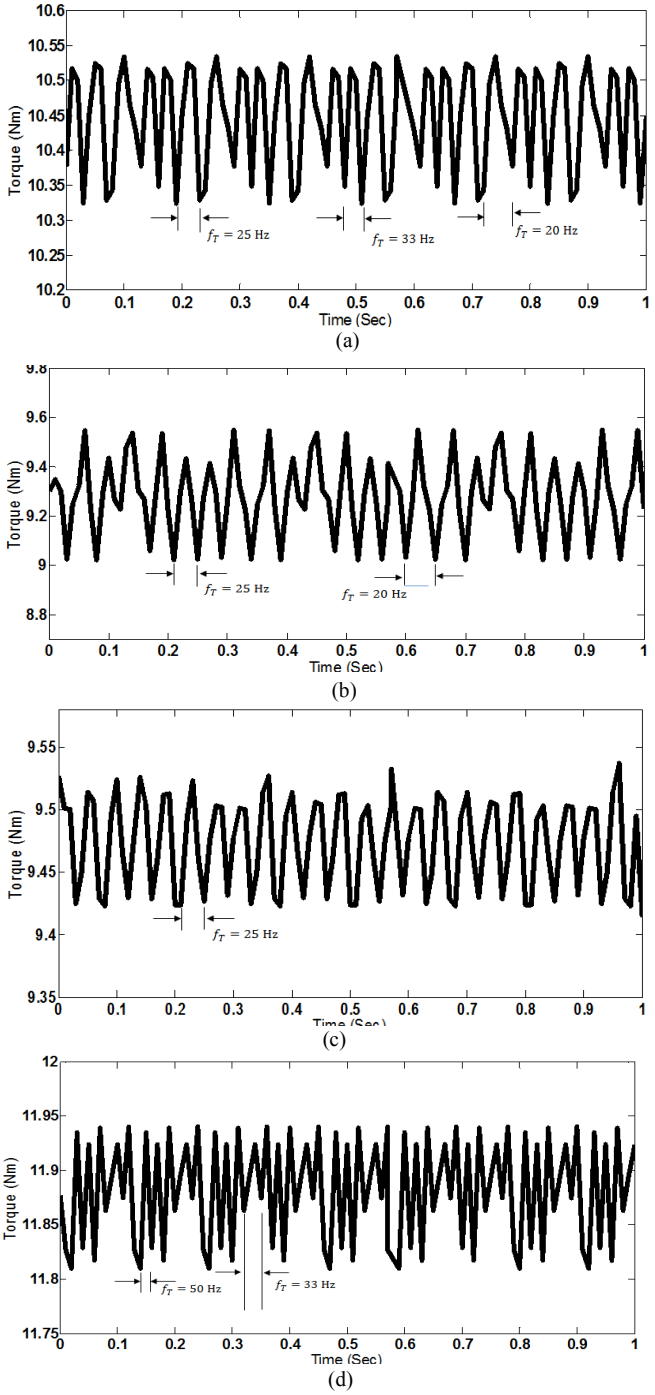

Fig.7. Experimental torque profile at full-load with loss of two non-adjacent phases, (a) DL-14/15, (b) DTL-14/15, (c) DL-13/15, (d) DTL-13/15

Furthermore, the experimental torque profiles measured in time domain of FPIMs with proposed mixed winding layouts operating with loss of two adjacent phases show oscillations are about 11.1 Hz and 9.1 Hz for DTL-14/15 and about10 Hz and 14.3 Hz for DTL-13/15. At the other hand, with loss of two non-adjacent phases the experimental torque profiles show oscillations of about 20 Hz, 25 Hz and 33 Hz for the conventional DL-14/15, and only of about 25 Hz for the conventional DL-13/15. For the proposed FPIM with DTL-14/15 winding layout, the torque oscillations are about 20 Hz and 25 Hz, and about 33 Hz and 50 Hz for the proposed FPIM with DTL-13/15 winding layout.

B. Torque Ripple Analysis

The torque ripples are mainly due to the induced rotor currents with non-fundamental frequencies that correspond to other sequences [14]. For a five-phase system, the number of available sequences is four and one zero sequence [14]. Both fundamental and third sequences are rotating in the forward direction. The fourth sequence is backward of the first sequence, while the second sequence is backward of the third sequence. The determination of induced frequencies in rotor currents is well detailed in [14], [15], [16]. The % experimental and simulation torque ripples for healthy and faulty operations which are given from Table III to Table VI were obtained at rated load.

TABLE III
HEALTHY FPIMs

Description	Experiment T_{av}	FEM T_{av}	Experiment T_{ripple}	FMM T_{ripple}
DL-13/15	10.53 Nm	10.23 Nm	1.02 %	2.15 %
DL-14/15	10.00 Nm	9.98 Nm	1.09 %	1.75 %
DTL-13/15	11.81 Nm	12.14 Nm	0.90 %	1.07 %
DTL-14/15	11.66 Nm	11.90 Nm	0.75 %	0.86 %

TABLE IV
FAULTY FPIMs WITH LOSS OF PHASE "A"

Description	Experiment T_{av}	FEM T_{av}	Experiment T_{ripple}	FEM T_{ripple}
DL-13/15	11.51Nm	12.91 Nm	210.55 %	204.26 %
DL-14/15	10.27 Nm	11.07 Nm	199.02 %	189.71 %
DTL-13/15	11.95 Nm	13.75 Nm	139.36 %	124.40 %
DTL-14/15	11.81 Nm	13.51 Nm	132.54 %	114.62 %

TABLE V
FAULTY FPIMs WITH LOSS OF TWO ADJACENT PHASES

Description	Experiment T_{av}	FEM T_{av}	Experiment T_{ripple}	FMM T_{ripple}
DL-13/15	8.96 Nm	10.07 Nm	164.55 %	151.26 %
DL-14/15	6.54 Nm	7.16 Nm	180.25 %	191.07 %
DTL-13/15	10.34 Nm	11.92 Nm	94.45 %	89.84%
DTL-14/15	10.67 Nm	11.71 Nm	80.37 %	81.09 %

TABLE VI
FAULTY FPIMs WITH LOSS OF TWO NON-ADJACENT PHASES

Description	Experiment T_{av}	FEM T_{av}	Experiment T_{ripple}	FMM T_{ripple}
DL-13/15	10.19 Nm	10.87 Nm	121.91 %	118.06 %
DL-14/15	9.53 Nm	10.21 Nm	107.08 %	112.48 %
DTL-13/15	10.54 Nm	12.06 Nm	49.18 %	48.03 %
DTL-14/15	10.18 Nm	11.65 Nm	41.63 %	45.62 %

The results from the above tables show that the torque ripples increase in both conventional and proposed mixed winding layouts when FPIMs operate under open-circuited faults. These increments in torque ripple are due to unbalanced MMF phase distribution as elaborated in previous paragraphs. From the same results, it is also observed that there is a reduction in torque ripple when employing the proposed mixed winding layouts. Under healthy operation the torque ripple reduction is about 29 % and 31 % for DTL-
14/15 and DTL-13/15, respectively. When operating with loss of one phase the drop in torque ripple is about 44 % for both DTL-14/15 and DTL-13/15. With loss of two adjacent phases the torque reduction is evaluated at 57 % and 65 % for DTL-14/15 and DTL-13/15, respectively. When operating with loss of two non-adjacent phases the torque ripple reduction is about 60 % and 61 % for DTL-14/15 and DTL-13/15, respectively. The fault-tolerance that exhibits the FPIMs with proposed mixed winding layouts operating under open–circuited faults is due to a better stator MMF distribution obtained by widening the phase spread from $\pi/5$ to $4\pi/15$, and by also having conductors that belong to two different phases in each and every single slot.

VI. CONCLUSION

This paper addressed the fault-tolerant ability of five-phase induction machines with mixed winding layouts to produce torque with less ripple contents. The practical and simulation results of five-phase IMs operating with loss of one phase then two adjacent phases and two non-adjacent phases have been presented and analysed. It has been noticed that under open-circuited faults, the torque ripples increased in both conventional and proposed winding topologies. Though there is loss of one or two adjacent or two non-adjacent phases the proposed five-phase IMs with mixed winding layouts, still have the edge to produce a better torque average with lesser ripple contents compared to its counterpart conventional double layer winding. The proposed idea in this paper means that the designer needs to make provision for enough space in the slots to accommodate insulation and avoid creating big space between coil sides in a slot. By doing so, the introduction of additional air-gap harmonic conductance are avoided. Further work will report on the acceleration torque of the proposed mixed winding layouts when operating under open-circuited faults.

VII. REFERENCES

[1] M. Muteba, A. A. Jomoh and D.V. Nicolae, " Torque ripple Reduction in five-phase induction machines using mixed winding configurations", *IEEE, XX International Conference on Electrical Machines-ICEM'201*2, Marseille, France.

[2] A. S. Abdel-Khalik and S. Ahmed, "Performance evaluation of a five-phase modular winding induction machine", *IEEE Trans, on Industrial Applications*, Vol.59. No.6, pp. 2654-2669, June. 2012.

[3] J. A. Riveros, A. G. Yepes, F. Barrero, J. D. Gandoy, B. Bogado, O. Lopez, M. Jones and E. Levis, " Parameter Identification of Multiphase Induction Machines With Distributed Windings- Part 2: Time-Domain Techniques. ". *IEEE Transaction on energy conversion*, Vol.27, NO4, DECEMBER 2012.

[4] L. Gao, J. E. Fletcher, and L. Zheng, "Low-Speed Control Improvements foe a Two-Level Five-Phase Inverter-Fed Induction Machine Using Classic Direct Torque Control. *IEEE Transaction on industrial electronics*, Vol.58, NO.7, July 2011.

[5] E. Levi, M. Jones, S. N. Vukosavic, and H. A. Toliyat, "Steady-State Modeling of Series-Connected Five-Phase and Six-Phase Two-Motor Drives. *IEEE Transactions on industry applications*, Vol.44, NO.5, Sep. / Oct. 2008.

[6] E. Levi, M. Jones, S. N. Vukosavic, A. Iqbal and H. A. Toliyat, "Modeling, Control, and Experimental Investigation of a Five-Phase Series-Connected Two-Motor Drive with Single Inverter Supply. *IEEE Transactions on industrial electronics*, Vol.54, NO.3, JUNE 2007.

[7] T. H. Liu, J. R. Fu, and T. A. Lipo, "A strategy for improving reliability of field oriented controlled induction drives," *1991 IEEE US Annu. Meet. Conf. Rec.*, vol. 1, pp. 449-455.

[8] H. A. Toliyat, S. P. Waikar and T. A. Lipo "Analysis and Simulation of Five-Phase Synchronous Reluctance Machines Including Third Harmonic of Airgap MMF. *IEEE Transactions on industry applications,* Vol.34, NO.2, March. / April. 1998.

[9] M. A. Alhamadi and N. A. Demerdash " Three-dimensional magnetic field computation by a coupled vector-scalar potential method in brushless DC motors with skewed permanent magnet mounts-the formulation and FE grids", 1994, *IEEE Transactions on Energy Conversion*, Vol.9, pp. 1-14.

[10] N. Demerdash, T. Nehl, O. Mohammed and F. Fouad " Nonlinear three dimensional magnetic vector potential finite element solution on field problems including experimental verification", 1981, *IEEE Transaction on Magnetics*, Vol. 17, pp. 3408-3410.

[11] A. Kameari "Regularization on ill-posed source terms in FEM computation using two magnetic vector potentials", 2004, *IEEE Transaction on Magnetics*, Vol. 40, pp. 1310-1313.

[12] R. Paul and K. V. I. S. Kaler "Comparison of the effective dipole method for the computation of the torque with the Maxwell's stress tensor method in non-lossy systems", *1990 IEEE Industry Application Annual Meeting.*

[13] Y. Zhao, Y. Tian, S. Udpa and S. Li "Investigation on boundary condition for magnetic vector potential applied in FEM for 3D electromagnetic computation", *2006, IEEE Antennas and Propagation Society International Symposium.*

[14] A. S. Abdel-Khalik , S. Ahmed , A. A. Elserougi and A. M. Massoud, "Effect of stator winding connection of five-phase induction machine on torque ripples", *IEEE Trans, on Mechatronics*, Vol.20. No.2, pp. 580-593, April. 2015.

[15] A. S. Abdel-Khalik , S. Ahmed , A. A. Elserougi and A. M. Massoud, "Effect of stator winding connection on Performance of five-phase induction machines", *IEEE Trans, on Industrial Electronics*, Vol.61. No.1, pp. 3-19, January. 2014

[16] J. R. Fu and T. A. Lipo, " Disturbance-free operation of a multiphase current-regulated motor drive with opened phase", *IEEE Trans, Ind. Appl.,* Vol. 30, No. 5, pp. 1267-1274, Sep./Oct. 1994.